

# Conformational Dynamics in the Acyl-CoA Synthetases, Adenylation Domains of Non-ribosomal Peptide Synthetases, and Firefly Luciferase

Andrew M. Gulick\*

Hauptman-Woodward Medical Research Institute and Department of Structural Biology, State University of New York at Buffalo, 700 Ellicott St., Buffalo, New York 14203-1102

*The results of numerous investigations on luciferase and other acyl adenylate synthetases indicate that large conformational changes occur in the protein when the specific substrates combine at the active site.* W. D. McElroy, M. DeLuca, J. Travis (1967)

*From a comparison of the allosteric manifestations of the overall reaction and partial reaction (b) it appears that the same conformational state (R), showing a greater affinity for CoA, catalyzes both the overall reaction and partial step (b), whereas the T-configuration, favored in the presence of PP<sub>i</sub>, seems to catalyze the ATP-forming step (reversal of partial reaction a).* J. Bar-Tana and G. Rose (1968)

These statements were made over 40 years ago about a family of enzymes that has recently garnered much attention. This family of ligases, which now includes acyl- and aryl-CoA synthetases, the adenylation domains of non-ribosomal peptide synthetases (NRPSs), and firefly luciferase, catalyzes the activation of a carboxylate substrate with ATP to form an acyl adenylate intermediate that is used in a diverse set of second partial reactions. The study of this family of adenyating enzymes has a long history, dating back to work in the 1950s with acyl-CoA synthetases. A decade later, biochemical studies of the reactions catalyzed by different members of this family allowed McElroy *et al.* (1) as well as Bar-Tana and Rose (2) to suggest that large conformational changes play a role in the catalysis of the complete two-step reaction. Bar-Tana and Rose even suggested that the two partial reactions of the acyl-CoA

**ABSTRACT** The ANL superfamily of adenyating enzymes contains acyl- and aryl-CoA synthetases, firefly luciferase, and the adenylation domains of the modular non-ribosomal peptide synthetases (NRPSs). Members of this family catalyze two partial reactions: the initial adenylation of a carboxylate to form an acyl-AMP intermediate, followed by a second partial reaction, most commonly the formation of a thioester. Recent biochemical and structural evidence has been presented that supports the use by this enzyme family of a remarkable catalytic strategy for the two catalytic steps. The enzymes use a 140° domain rotation to present opposing faces of the dynamic C-terminal domain to the active site for the different partial reactions. Support for this domain alternation strategy is presented along with an explanation of the advantage of this catalytic strategy for the reaction catalyzed by the ANL enzymes. Finally, the ramifications of this domain rotation in the catalytic cycle of the modular NRPS enzymes are discussed.

\*Corresponding author,  
gulick@hwi.buffalo.edu.

Received for review May 15, 2009  
and accepted July 16, 2009.

Published online July 19, 2009  
10.1021/cb900156h CCC: \$40.75

© 2009 American Chemical Society

synthetases might be catalyzed by different conformational states. Forty years later, the structural biochemistry of these enzymes has been thoroughly investigated, and it is remarkable how prescient these early statements appear to have been. This Review describes the biochemical and structural data for a novel catalytic mechanism used by these enzymes and the chemical requirements of the two-step reactions that benefit from this strategy.

**ANL Family of Adenylating Enzymes.** The activation of biological carboxylates as thioesters with CoA has been known for over 60 years. The conversion of acetate to acetyl-CoA was first described by Lipmann (3) using a partially purified bacterial enzyme. The mechanism proceeded through an acetyl-phosphate intermediate, which was then converted to acetyl-CoA. A second enzymatic mechanism for the synthesis of acetyl-CoA was identified in the next decade by Berg (4), who purified from baker's yeast a protein he called aceto-CoA kinase that activated acetate not through an acyl-phosphate intermediate but rather through an acyl-adenylate. This study demonstrated the exchange of  $^{32}\text{P-PP}_i$  into ATP in an acetate-dependent manner and that the acetyl-AMP intermediate could react with  $\text{PP}_i$  for the formation of ATP or with CoA to form acetyl-CoA and AMP. The formation of acetyl-AMP from ATP and acetate occurred in the absence of CoA, demonstrating the independence of the two partial reactions. Rigorous attempts to separate the active fraction into two distinct enzymes that catalyzed the adenylation and the thioester-forming reactions were unsuccessful, and a single enzyme was proposed to be responsible for the production of acetyl-CoA, AMP, and  $\text{PP}_i$  directly from acetate, ATP, and CoA, proceeding through the acetyl-AMP intermediate. A related medium chain acyl-CoA synthetase was subsequently demonstrated to use a bi-uni-uni-bi ping pong mechanism (2). Such ping pong kinetics have since been confirmed for many acyl-CoA synthetases, including enzymes with specificity for acetate (5), malonate (6), long chain fatty acids (7), and more complex aryl acids (8, 9).

The possibility that this adenylating enzyme family contained members beyond the acyl- and aryl-CoA synthetases was raised as early as 1967 by McElroy and colleagues, who noted the functional similarities of the acyl-CoA synthetases with firefly luciferase, as well as with the reaction of pantoic acid in pantetheine cofactor biosynthesis and the activation of amino acids by

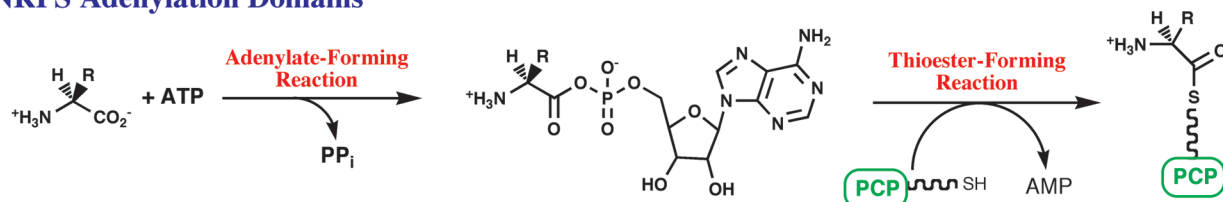
amino acyl-tRNA synthetases (1). As sufficient sequence information became available, several reports (10, 11) noted that the acyl-CoA synthetases and luciferase enzymes shared numerous conserved sequence motifs. The amino acyl-tRNA synthetase and pantothenate synthetase enzymes, although functionally similar, share no sequence homology. In the late 1980s, several multidomain proteins that produce bacterial peptide antibiotics or siderophores were also identified that share similar sequence motifs (12–14). This new class of modular enzymes became known as non-ribosomal peptide synthetases (NRPSs) and formed the third subfamily of this adenylating enzyme superfamily.

We and others have referred to this enzyme family as the “adenylate-forming superfamily” of enzymes or the “acyl-AMP-forming family of adenylation enzymes”. Neither of these names is particularly satisfying as other acyl-adenylating enzymes exist that do not belong to this family. Using the description of divergent superfamilies described by Gerlt and Babbitt (15), luciferase, acyl-CoA synthetases, and NRPS adenylation domains comprise a mechanistically diverse enzyme superfamily. The enzymes share ~20% sequence identity, are structurally homologous, and catalyze different overall reactions, while sharing a conserved mechanistic step, the adenylation partial reaction. Other adenylate-forming enzymes, such as the amino acyl-tRNA synthetases (16) or the NRPS-independent siderophore (NIS) adenylating enzymes (17), do not belong to this enzyme superfamily and are simply unrelated enzymes that catalyze a similar overall reaction.

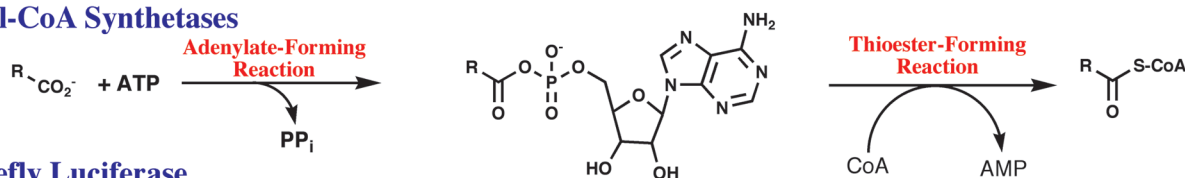
In the interests of providing a clear way to describe the enzyme superfamily that is the focus of this Review, I propose a new designation of the “ANL superfamily of adenylating enzymes”. This name is derived from the three main subfamilies, namely, the Acyl-CoA synthetases, the NRPS adenylation domains, and the Luciferase enzymes.

**Functional Diversity and Substrate Specificity in ANL Adenylating Enzymes.** Although distinct in the overall reactions catalyzed, the enzymes within all three subfamilies use a two-step reaction to first activate a carboxylate substrate by reacting with ATP to form the acyl-adenylate and inorganic  $\text{PP}_i$  (Figure 1). The adenylate, a high-energy acid anhydride, provides the activation energy for the second partial reaction. For the acyl-CoA synthetases and NRPS adenylation domains, a pantetheine thiol group attacks the carboxylate carbon, dis-

## NRPS Adenylation Domains



## Acyl-CoA Synthetases



## Firefly Luciferase

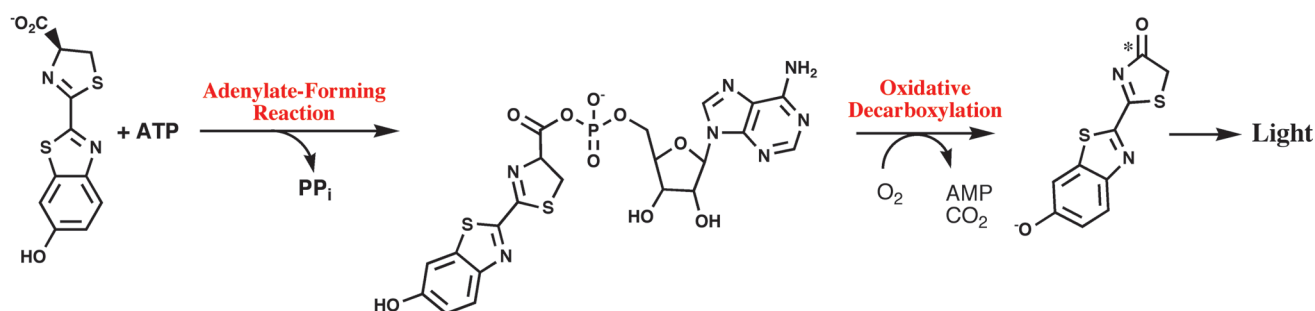


**Figure 1.** Reactions catalyzed by the ANL superfamily of adenyating enzymes. Chemical reactions catalyzed by the three subfamilies of the ANL adenyating enzymes. All three reactions include an initial, adenylate-forming reaction to form an acyl-, amino acyl-, or aryl-adenylate with the release of inorganic pyrophosphate. The adenylate intermediate reacts in a second partial reaction to release AMP. For NRPS adenylation domains, the pantotheine cofactor bound to an NRPS peptidyl carrier domain is represented by the linker and SH group.

placing the AMP leaving group, in the second half of the reaction. The hydrolysis of ATP in the first partial reaction therefore creates a higher energy adenylate intermediate that is utilized for the thioester-forming step. In the reaction catalyzed by luciferase, the activated luciferyl-adenylate undergoes an oxidative decarboxylation that results in the formation of an intermediate that subsequently decomposes within the enzyme active site to yield a photon of light. As described below, the unique chemical properties of these reactions have been facilitated by an interesting catalytic mechanism.

Many excellent reviews have been written describing the fascinating modular architecture of the NRPS enzymes (18–21), and these enzyme assembly lines will be described only briefly here. The multidomain NRPS enzymes generally contain a single module for the incorporation of each amino acid into the peptide product (Figure 2). During synthesis, the amino acid and peptide intermediates are bound to the pantotheine cofac-

tor of an integrated peptidyl carrier protein domain (22, 23). Within each module is an adenylation domain responsible for activating the amino acid substrate and transferring it to the pantotheine cofactor of the neighboring carrier protein domain. Finally, a condensation domain is required in all modules except the first to catalyze peptide bond formation and transfer the peptide from an upstream to a downstream carrier protein domain, increasing the peptide length by a single residue. This assembly line biosynthesis terminates with a thioesterase domain that cleaves and often cyclizes the peptide product. Reflecting the diversity of the peptide products that are produced, some NRPS proteins contain additional internal catalytic domains that are responsible for epimerization or N-methylation of the constituent amino acids. The ACV synthetase enzyme (24), for example, is a three-module protein involved in the synthesis of isopenicillin N, a  $\beta$ -lactam antibiotic. The ACV synthetase NRPS produces a tripeptide from

## ACV Synthetase

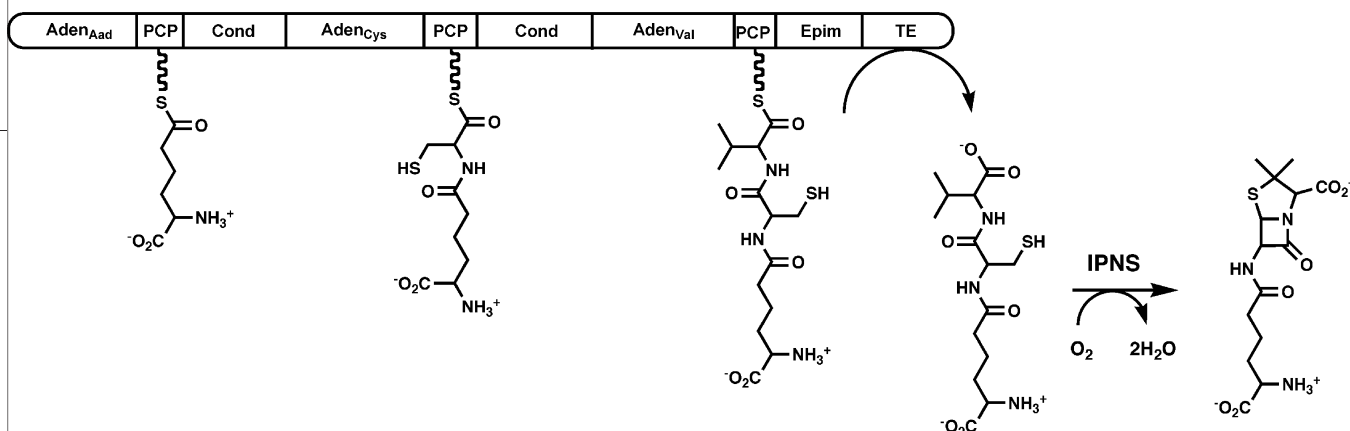


**Figure 2.** Modular organization of the non-ribosomal peptide synthetases. A schematic representation is shown of the ACV synthetase, a three-module protein that is responsible for the synthesis of the linear tripeptide of  $\alpha$ -amino adipic acid (Aad), cysteine, and valine. The linear peptide is subsequently cyclized by the enzyme isopenicillin N synthase. Module 1 contains the adenylation domain and PCP for Aad. Module 2 contains the adenylation and PCP domain for cysteine, as well as the condensation domain that forms the peptide bond between Aad and cysteine. The third module contains the adenylation and PCP domain for valine, an epimerization domain that converts L-valine to D-valine, and a condensation domain that transfers the upstream dipeptide to D-valine. The protein terminates with a thioesterase domain that releases the tripeptide.

$\alpha$ -amino adipic acid, cysteine, and valine that is then cyclized by the isopenicillin N synthase (25).

The choreography that delivers the substrate bound to the NRPS carrier protein domain to the neighboring catalytic domains is undoubtedly complex and is not clearly defined. Recent studies using alanine-scanning mutagenesis have defined the binding surface used by the *E. coli* EntB PCP domain for interactions with its functional partners, EntF and EntD (26, 27). Additionally, NMR studies have demonstrated that both the PCP domain and the catalytic domains will undergo local conformational rearrangements during their interactions (28–30). In particular, these studies suggest that the PCP domains are dynamic and can adopt multiple conformations and that the catalytic domains are able to stabilize one of the conformations selectively for a functional interaction. Nonetheless, these conformational changes are limited in scale, and it appears from a recent multidomain NRPS structure (31) that more significant conformational rearrangements are required for the proper delivery of amino acyl and peptide substrates to the different catalytic centers.

NRPS adenylation domains can be subdivided

into two classes. Most NRPS adenylation domains are integrated into the catalytic module (Figure 2) and activate and load the amino acid on the pantetheine cofactor of an adjacent carrier domain, referred to alternatively as the thiolation domain and the PCP domain (22). Other NRPS adenylation domains, however, are self-standing and transfer the amino acyl substrate *in trans* to a separate amino acyl carrier domain. In many cases these isolated adenylation domains load an acyl or aryl capping group that initiates the NRPS peptide (32).

The substrates of the acyl- and aryl-CoA synthetase subfamily of the ANL enzymes are chemically diverse, ranging in size from small acids such as acetate and propionate to medium- and long-chain fatty acids and aromatic compounds. The aryl-CoA ligases have been identified in a variety of pathways for the degradation of aromatic compounds, as well as for the biosynthesis of plant metabolites (33).

A subfamily of fatty acyl-AMP ligases (FAALs) has been characterized by Gokhale and colleagues (34, 35). These enzymes share functional features with both the acyl-CoA synthetases and the NRPS adenylation domains. The acyl substrate of these enzymes are fatty acids that are used in the formation of complex lipopeptides, some of which play a role in virulence. Unlike the acyl-CoA synthetases, however, the enzymes of this family transfer the activated fatty acid from the adenylate directly to the pantetheine cofactor of an acyl carrier protein of an NRPS or polyketide synthase cluster (34). In this latter regard, these enzymes share more in common with the NRPS adenylation domains than with the fatty-acyl CoA synthetases. In particular, these enzymes are reminiscent of the self-standing aryl activating of many NRPS siderophore clusters (36) that activate sa-

### KEYWORDS

**ANL superfamily of adenylating enzymes:** An enzyme superfamily containing acyl- and aryl-CoA synthetases, the adenylation domains of NRPS modular proteins, and firefly luciferase.

**Modular enzyme:** Enzymes that contain multiple catalytic domains joined in a single polypeptide to catalyze sequential biosynthetic steps.

**Non-ribosomal peptide synthetase:** A modular enzyme that is responsible for the synthesis of peptide antibiotics and peptide siderophores. The amino acid and peptide intermediates are covalently bound to a peptide carrier domain through a pantetheine cofactor during synthesis by the individual catalytic domains.

**Domain alternation:** A catalytic strategy where an enzyme uses large-scale domain rotations to catalyze different steps of a multistep reaction. The conformational changes are distinct from simple opening and closing of an active site loop.

**Peptidyl carrier protein:** A four-helix dynamic protein domain that contains a pantetheine cofactor bound to a conserved serine residue, on which amino acid and peptide intermediates are bound during NRPS synthesis.

TABLE 1. Conserved sequence motifs

Core <sup>a</sup>	Motif <sup>b</sup>	Consensus sequence <sup>c</sup>	Position <sup>d</sup>	Role
A1		$\theta(S/T)\phi x(E/Q)\theta$	Leu30	Structural role. Caps a helix at N-terminus of the protein
A2		$(R/K/F)\theta G\theta$	Arg76	Structural role. Torsion angles enforce a glycine at position 78
A3	I	$\theta\theta x(S/T)(S/T/G)G(S/T)TGxPK$	Ile158	Phosphate-binding loop, orienting the $\beta,\gamma$ -phosphates
A4		$\phi$	His207	Active site aromatic residue that alternates conformation in the two enzyme states and caps a helix that forms part of the acyl-binding pocket
A5	II	$\phi(G/W)x(A/T)E$	Tyr304	Initial aromatic residue stacks against adenine ring of ATP, glycine, or tryptophan, forms wall of active site, Glu binds the $Mg^{2+}$ ion
A6		$GEx_{10-14}GY$	Gly351	Structural role. Forms a portion of the distorted $\beta$ -sheet of the N-terminal domain
A7	III	$(S/T)GD$	Ser383	The aspartic acid of this motif binds the ribose hydroxyls of ATP and is 100% conserved
A8		$Rx(D/K)x_cG$	Arg400	The arginine interacts with ribose hydroxyls. The aspartic acid (or rarely lysine) is the hinge residue. The glycine abuts the pantetheine tunnel in the thioester-forming conformation
A9		No conservation within larger family		
A10		$Px4GK\theta x(R/K)$	Pro486	The first lysine (Lys492) is present at the active site in the adenylate-forming conformation

<sup>a</sup>Core sequence as defined by Marahiel *et al.* (38) for NRPS adenylation domains. <sup>b</sup>Motif defined by Chang *et al.* (37) for aromatic adenylate forming ligases. <sup>c</sup>Single amino acid code,  $\theta$  is used for medium aliphatic amino acids (alanine, valine, leucine, isoleucine, methionine).  $\phi$  is used for aromatic amino acids (phenylalanine, tyrosine, histidine, tryptophan). <sup>d</sup>Position is provided for the first amino acid residue of the motif in the representative enzyme 4-chlorobenzoyl-CoA ligase.

licylate or 2,3-dihydroxybenzoate and transfer the aromatic acid to an aryl carrier protein domain (32).

As more members of the adenylate-forming family of enzymes were identified, several groups proposed a number of conserved sequence motifs to be important for catalytic activity. The first identified sequence was a serine-, threonine-, and glycine-rich motif (10). This region was deemed a signature sequence for the ANL enzyme family and was designated Motif I. Two additional regions (Motif II and Motif III) were also identified on the basis of sequence conservation (37). A more detailed comparison of the conserved regions exclusively within the NRPS adenylation domains identified 10 conserved regions, named A1–A10 (38). The determination of crystal structures of members of this enzyme family allowed a preliminary understanding of the roles of these conserved motifs in the catalytic residues (Table 1). Interestingly, the conservation of several regions that were located at some distance from the active site of the first structures can now be rationalized on

the basis of the domain rearrangements described below.

**Structural Studies of ANL Family of Adenylating Enzymes.** As of July 2009, there are 47 crystal structures of members of the ANL adenylating enzyme family deposited in the Protein Data Bank (Table 2). These structures represent 16 different proteins and have been crystallized in a variety of liganded states, providing a detailed view of the catalytic strategy used by this enzyme family.

The first crystal structure of a member of the adenylate-forming family of enzymes was of firefly luciferase from *P. pyralis* (39). This structure identified an overall two-domain architecture with a larger N-terminal domain composed of the first 430 residues and a smaller C-terminal domain composed of the final 120 residues (Figure 3, panel A). The larger domain contained an  $\alpha\beta\alpha\beta\alpha$  domain structure with two large eight-stranded  $\beta$ -sheets that surround two  $\alpha$ -helices. The N-terminal domain ends with a distorted  $\beta$ -sheet. Fol-

**TABLE 2. Acyl-AMP forming adenylating enzymes that have been structurally characterized**

Protein	Organism	Conformation	PDB codes and ligands or mutant structure
Luciferase	<i>P. pyralis</i>	Intermediate	1LCI, unliganded; 1BA3, bromoform
PheA	<i>B. brevis</i>	Adenylation	1AMU, AMP + phenylalanine
DhbE	<i>B. subtilis</i>	Adenylation	1MDF, unliganded; 1MD9, AMP + DHB; 1MD8, DHB-AMP adenylate
Acs	<i>S. enterica</i>	Thioester	1PG4, adenosine-5'-propylphosphate + CoA; 1PG3, same ligands, acetylated on Lys609; 2P2F, acetate, AMP, COA; 2P20, R584A; 2P2B, V386A; 2P2J, K609A; 2P2M, R194A; 2P2Q, R584E
Acs	<i>S. cerevisiae</i>	Adenylation	1RY2, AMP
CBL	<i>Alcaligenes</i> sp. AL3007	Adenylation	1T5S, unliganded; 1T5D, 4CB; 2QVX, 2QVY, I303G; 2QVZ, 2QV0, I303A; 3CW8, 4CB-AMP; 3DLP, D402P
Fatty Acs	<i>T. thermophilus</i>	Thioester	3CW9, 4CPh-CoA + AMP
		Aden/Intermed	1ULT, unliganded
Luciferase	<i>L. cruciata</i>	Thioester	1V25, AMPPNP; 1V26, Myristyl-AMP
		Adenylation	2D1Q, AMP; 2D1R, oxyluciferin + AMP; 2D1S, <i>N</i> -(dehydrolyciferyl) sulfamoyl adenosine; 2D1T, T2171
Benzoyl-CL	<i>B. xenovornans</i>	Adenylation	2V7B, benzoic acid
Med. Acs	<i>H. sapiens</i>	Adenylation	3C5E, ATP; 2V7E, AMP; 3DAY, AMPPNP; 3EYN, CoA
		Thioester	3B7W, unliganded; 3EQ6, butyryl-CoA + AMP
SrfA-C	<i>B. subtilis</i>	~Adenylation	2VSQ, Leu. Multidomain NRPS
DltA	<i>B. cereus</i>	Adenylation	3DHV, alanyl-AMP; 3FCC, Mg-ATP; 3FCE, Ca-ATP
DltA	<i>B. subtilis</i>	Thioester	3E7W, AMP; 3E7X, AMP
AAE	<i>M. acetivorans</i>	Thioester	3ETC, unliganded
FAAL28	<i>M. tuberculosis</i>	N-Terminal domain	3E53, unliganded
		only	
Fatty Acs	<i>A. fulgidus</i>	Intermediate	3G7S, unliganded

lowing a short disordered loop in the luciferase structure, the C-terminal domain begins with an antiparallel  $\beta$ -sheet that contained two strands, followed by a central three-stranded  $\beta$ -sheet that was surrounded by helices. The residues connecting the two domains form the A8 motif (Table 1) and are collectively referred to as the A8 loop. Luciferase was crystallized in the absence of ligands. The conserved sequence motifs (40) were used to propose a location of the enzyme active site. In particular, the glycine- and serine-rich Motif I was located at the interface between the N- and C-terminal domains. Conti *et al.* (39) note that the cleft is likely “too big to accommodate the substrates” and predict closure of the interface upon substrate binding.

As noted above, early experiments predicted a large conformational change for acyl-CoA synthetases and luciferase (1) on the basis of tritium exchange and thermal inactivation in the presence and absence of ligands. A conformational change was also invoked to explain the stabilization of phenylacetyl-CoA ligase (41). The crystal structure of firefly luciferase thus provided a structural framework to envision this large conformational change. The single structure, however, provided only an initial look at the protein and many additional structural studies were necessary to understand the full conformational mechanism.

The structure of an initiating NRPS adenylation domain, the phenylalanine activating domain of gramicidin synthetase S (GrsA), was determined the following year (42). Importantly, this structure was determined in the presence of the amino acyl substrate phenylalanine and a molecule of AMP (Figure 3, panel B), confirming the predicted location of the active site. The C-terminal domain was rotated by  $\sim 90^\circ$  compared to the orientation seen in the luciferase structure. A universally conserved lysine from the A10 region formed hydrogen bonds to the ribose ring oxygen, the 5'-bridging oxygen, and a carboxylate oxygen of phenylalanine. This suggested a possible catalytic role for this lysine, which was indeed supported by prior biochemical studies of tyrocidin synthetase (40).

These initial structures provided the foundation for a number of studies that investigated the roles of catalytic or substrate specificity residues. In particular, the interaction of the C-terminal lysine from the A10 region (Table 1) was studied by mutagenesis in both luciferase (43) and PrpE, a propionyl-CoA synthetase (44). No activity could be detected for the complete reaction of the K592E mutant of PrpE, for example, and activity was reduced by over 4 orders of magnitude for the reverse of the adenylation reaction; the rate of production of propionyl-CoA from the propionyl-AMP intermediate, however, was reduced by only a factor of 2. These stud-

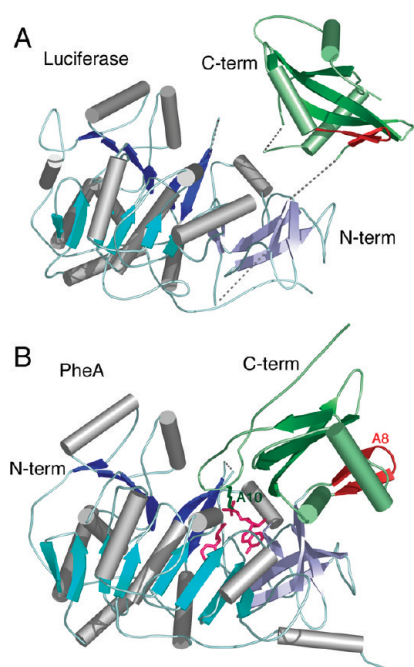


**Figure 3.** Crystal structures of A) firefly luciferase and B) PheA adenylation domain, the first two members of the ANL superfamily of enzymes to be characterized by crystallography. The proteins are aligned on the basis of the N-terminal domains. The structure of luciferase (1LCI) displayed an open conformation with few interactions between the N- and C-terminal domains. Several disordered loops are indicated with dashed lines. PheA was cocrystallized in the presence of ATP and phenylalanine (1AMU) and revealed a molecule of AMP and phenylalanine in the active site (pink). The A8 loop, that follows the hinge for domain alternation is shown in red while the A10 lysine that is conserved throughout the entire family is shown in green. In both panels, the N-terminal domain is represented with  $\beta$ -sheets of different shades of blue, and the C-terminal domain is shown in green.

ies demonstrated a role of this residue specifically in the adenylation partial reaction.

Subsequent to the structural characterization of PheA, a number of additional structures of enzymes in this family were determined that demonstrated a similar tertiary structure and a similar conformational orientation between the N- and C-terminal domains. These structures included DhBE, the self-standing adenylation domain from the bacillibactin NRPS cluster (45), yeast acetyl-CoA synthetase (46), two enzymes that catalyze aryl-CoA synthesis that are involved in the metabolic breakdown of 4-chlorobenzoate (47) and benzoic acid

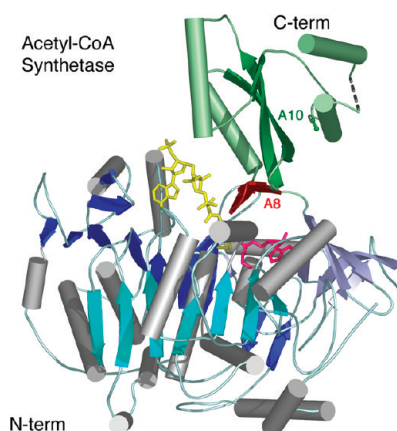


**Figure 4.** Crystallographic structure of acetyl-CoA synthetase. The structure is shown of bacterial acetyl-CoA synthetase (1PG4). The enzyme is oriented as other family members are in Figure 3 and includes the ligands adenosine-5'-propylphosphate (pink) and CoA (yellow). The CoA nucleotide binds on the surface of the N-terminal domain while the pantetheine passes into the enzyme active site via the *pantetheine tunnel*. The A8 loop that follows the hinge is shown in red. The  $\alpha$  and  $\beta$  positions of Lys609, the A10 lysine, are shown in green. The N- and C-terminal domains are colored as in Figure 3.

(48), luciferase from *L. cruciola* (49), and the enzyme DltA from *B. cereus*, which is involved in the activation of alanine for subsequent alanylation of teichoic acid in cell wall biosynthesis of Gram-positive bacteria (50, 51). These structures were all determined in the absence of ligands or in the presence of the acyl substrate, the adenylate, or AMP. Notably, none of these structures contained a bound CoA or thiol acceptor for the second partial reaction (Table 2).

Insights into CoA binding were derived from the crystallization of a bacterial acetyl-CoA synthetase (Acs) bound to adenosine-5'-propylphosphate, a non-hydrolyzable mimic of the adenylate intermediate, and CoA (52). This structure, which appeared to show the enzyme poised to catalyze the thioesterification reaction, located the nucleotide of CoA at the surface of the protein with the pantetheine portion of CoA passing through a *pantetheine tunnel* that runs between the N- and C-terminal domains to enter the mostly buried adenylate binding site.

The most intriguing feature of this structure was that the C-terminal domain of Acs adopted a dramatically different conformation compared to that seen in the prior structures of PheA and DhBE (Figure 3, panel B). The

C-terminal domain of Acs packed against the N-terminal domain forming a more lobular enzyme (Figure 4). Multiple interactions were observed between the two domains and between the C-terminal domain and the reaction intermediates. In this conformation, the loop containing the A10 lysine residue is 25 Å from the active site. In contrast, the A8  $\beta$ -sheet that initiates the C-terminal domain was rotated into the active site. The luciferase C-terminal domain, which was also observed in a conformation than observed in PheA, did not make any interactions with the N-terminal domain and did not seem to be a functionally relevant conformation.

The biochemical data implicating the A10 lysine from the C-terminal domain in catalyzing the adenylate-forming reaction specifically (43, 44) and the structural observation of this new conformational state of Acs bound to CoA provided preliminary support for a novel catalytic strategy (52). In this proposed catalytic strategy, the members of this adenylate-forming family would adopt the PheA-like structure to catalyze the adenylation partial reaction. Upon formation of the adenylate and the release of pyrophosphate, the C-terminal domain would rotate to the orientation observed in the bacterial Acs to form a second conformation that would be used to catalyze the thioester-forming reaction. We adopted the term *domain alternation*, which had been used to describe a large-scale domain rearrangement in methionine synthase (53), to describe this mechanism.

The crystal structures of several other members of this enzyme family have since been determined in this conformation. These structures include the long chain fatty acyl-CoA synthetase from *T. thermophilus* (54), DltA from *B. subtilis* (55), and an acyl-adenylating enzyme from the methanogenic bacteria *Methanosarcina acetivorans* (56). Interestingly, while the Acs structure contained CoA, these latter structures did not contain bound coenzyme A, although in the case of the fatty acyl-CoA synthetase, CoA was included in the crystallization conditions yet was not bound in the crystal structure.

In the past year, two examples of a single enzyme being crystallized in both conformations have been reported. The 4-chlorobenzoyl-CoA ligase (4CBL) from *Alcaligenes* sp. AL3007 was the subject of extensive structural and kinetic evaluation, as will be discussed below. As part of this study, the enzyme was trapped in both the adenylate-forming conformation bound to the adenylate intermediate as well as to a complex of AMP

and the product analogue 4-chlorophenacyl-CoA (57). More recently, the structure of the human medium chain Acyl-CoA synthetase has also been determined in both conformational states (58). These alternate structures demonstrate that the domain rotation is a dynamic feature of the ANL enzymes and does not simply reflect differences in tertiary organization between different superfamily members.

Not surprisingly, crystallization of these conformationally flexible enzymes has been challenging, and several of the deposited structures exhibit significant disorder in the C-terminal domain. Indeed, a recent structure of a FAAL (34, 59) required the removal of the C-terminal domain altogether to achieve crystallization. As with all structural studies, the careful selection of appropriate inhibitors can support the crystallization of enzymes trapped in relevant conformations. The use of alkyl phosphate esters (52) or adenosyl sulfamate analogues (49) as mimics of the adenylate intermediate or a substituted phenacyl-CoA thioether (57) as a mimic of the CoA thioester product has enabled the determination of some of the highest resolution structures of members of this conformationally dynamic enzyme family.

**Active Site of the Acyl-AMP Forming Adenylating Enzymes.** Acs (52, 60), 4CBL (57), DltA (50, 51, 55), and a human medium chain acyl-CoA synthetase (58) have now been studied structurally with numerous ligand complexes or structures of site-directed mutants. These structures give insights into the catalysis of the individual reactions and illustrate residues responsible for substrate binding. The active sites of these four proteins will be described as representative members of the family.

The carboxylate substrate binds in a pocket located within the N-terminal domain (Figure 3, panel B and Figure 4). The residues that form the binding pocket are quite diverse, reflecting the differences in substrate specificity between different enzyme family members. In fact, we have recently noted (56) that the core of the N-terminal domain of five structurally characterized acyl-CoA synthetases contains only 14 conserved residues (out of 250). Interestingly, a conserved glycine is observed throughout the superfamily except in acetyl- and propionyl-CoA synthetase where this glycine is replaced by a tryptophan residue that truncates the acyl binding pocket for the smaller substrates (47).

The amino acyl binding pocket of NRPS adenylation domains is better characterized than the acyl-CoA syn-



thetase pockets. The substrate  $\alpha$ -amino group is positioned by a conserved aspartic acid residue that directs the amino acid side chain into a pocket that is chemically complementary to the specific substrate. This feature of the adenylation domain binding pocket has allowed the clustering (61–63) and prediction (64) of specificity of NRPS adenylation domains.

The ATP binding site contains several highly conserved motifs that are present in all family members and perform similar roles in positioning the nucleotide (Figure 5, panel A). The aspartic acid residue of the A7/Motif III region, Asp385 of 4CBL, is universally conserved and interacts with one or both ribose hydroxyls. Fifteen residues downstream is the completely conserved arginine residue of the A8 motif, Arg400 in 4CBL, that also interacts with the ribose hydroxyls. An aromatic residue from the A5 motif, Tyr304 in 4CBL, stacks against the adenine base. Two recent structures, DltA and the human medium chain acyl-CoA synthetase (51, 58), illustrate the interactions that occur between protein and the triphosphate moiety. The Motif I residues that surround the  $\beta$ - and  $\gamma$ -phosphates of the human medium chain acyl-CoA synthetase (Figure 5, panel B) are well-conserved, suggesting that the ATP binding position will be similar in all family members.

The structure of DltA bound to ATP was recently determined and compared to previously characterized structures in the adenylation-forming conformation (51). The authors note that even within this conformation, differences of as much as  $40^\circ$  exist in the orientation of the C-terminal domain. The different orientation causes the invariant A10 lysine residue to interact with different ligand atoms, including the bridging oxygen between the ribose and phosphate and a carboxylate oxygen in PheA (42) and DhbE (45) or a  $\beta$ -phosphate oxygen in the medium chain acyl-CoA synthetase (58) or DltA (51). The authors raise the intriguing possibility that the ANL enzymes adopt a preadenylation state bound to ATP and a postadenylation state upon completion of the adenylation partial reaction. The A10 lysine residue is proposed to track the accumulation of negative charge on the initial attack complex, the transition state for adenylation formation, and finally to the pyrophosphate product prior to product release.

The CoA binding site can be divided into two regions, a nucleotide binding site that is located on the surface of the protein (Figure 5, panel C), and the previously mentioned pantetheine tunnel that runs between

the two domains. The tunnel contains a  $\beta$ -sheet-like interaction that occurs between the conserved glycine on the A8 loop and the  $\beta$ -alanine group of the pantetheine.

In the three protein structures bound to CoA in a productive conformation, the CoA nucleotide moiety is located in different positions (52, 57, 58). The adenine group of the CoA in the structures of the two acyl-CoA synthetases interacts most closely with the N-terminal domain, while the nucleotide moiety of the CoA ligand in 4CBL binds primarily to the C-terminal domain. In 4CBL, it is sandwiched between two aromatic side chains that are well conserved within other 4CBL enzymes (9) but not in the larger subfamily of acyl-CoA synthetases.

Catalysis of the thioester-forming reaction likely requires the deprotonation of the thiol of CoA to increase the nucleophilicity for attack on the carboxylate in the adenylation intermediate. Surprisingly, no conserved residues were identified in the area surrounding the CoA thiol. Instead, the enzymes may use the helix dipole of the helix that starts with the A4 aromatic residue to provide a positive dipole that could reduce the  $pK_a$  of the thiol (9).

#### Kinetic Evidence for the Domain Alternation

**Hypothesis.** The observations of the distinct structures support the domain alternation hypothesis; however, kinetic studies have been equally important for understanding the catalytic mechanism. In particular, these studies support the involvement of residues from the opposite faces of the C-terminal domain in the distinct partial reactions and identify the catalytic advantage that is gained by the domain alternation.

Following the original experiments on luciferase and PrpE (43, 44), studies have since been performed with all three subfamilies of the acyl-AMP forming adenylation enzymes that support the hypothesis that the two C-terminal conformations are used for the different partial reactions. Mutagenesis studies with luciferase (65), Acs (60), and the EntE self-standing adenylation domain (66) all demonstrate that residues on the A8 loop are important specifically for the thioester-forming partial reaction. As the A8 loop is rotated into the active site only in thioester-forming conformation, this supported the use of the conformation observed with Acs for the thioester-forming reaction.

To analyze more rigorously the effects of mutations on this enzyme family, the 4CBL enzyme was extensively mutated and subjected to kinetic analyses (9)

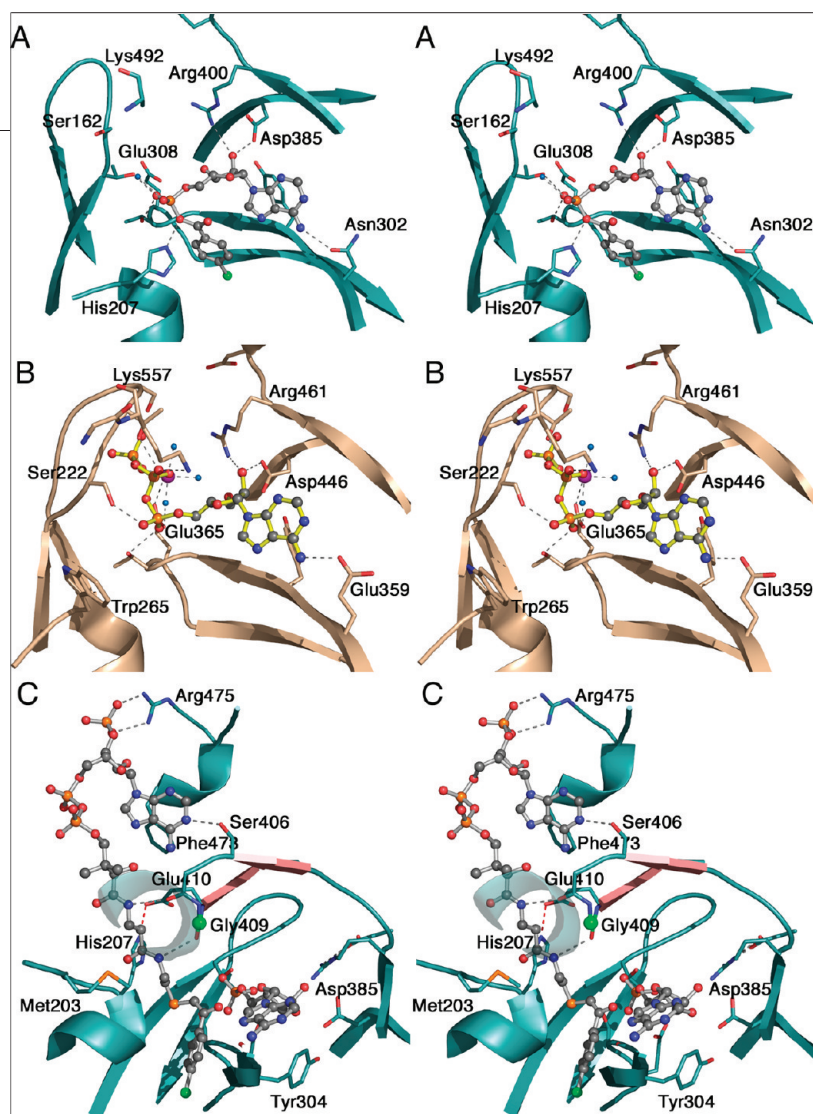


**Figure 5.** Active site and binding interactions of the ANL enzymes. **A)** Aryl-AMP binding site of 4CBL determined in the adenylate-forming conformation (3CW8). Conserved residues that interact with the adenylate are shown. Also interacting with the  $\alpha$ -phosphate are Thr161, from the P-loop, and Thr307. Tyr304, behind the adenine ring, is unlabeled. The side chain of the A10 lysine, Lys492, was disordered beyond C $\beta$ . **B)** ATP binding site of medium chain Acyl-CoA synthetase in the adenylate-forming conformation (3C5E). The interaction of the glycine- and serine/threonine-rich P-loop with the triphosphate of ATP is clearly demonstrated. The Mg<sup>2+</sup> ion, which bridges the  $\beta$ - and  $\gamma$ -phosphates, is shown in purple. Pairs of homologous residues between mAcS and 4CBL are (mAcS listed first with 4CBL residue in parentheses): Ser222 (Thr161), Thr223 (Ser162), Trp265 (His207), Glu359 (Asn302), Tyr361 (Tyr304), Thr364 (Thr307), Glu365 (Glu308), Asp446 (Asp385), and Arg461 (Arg400). **C)** Binding interactions between CoA and 4CBL observed in the thioester-forming conformation (3CW9). The CoA nucleotide binds on the surface of the 4CBL enzyme, with the nucleotide ring stacking against Phe473. The pantetheine passes to the interior of the protein where the CoA thiol can attack the adenylate intermediate. Here, the thioester bond is modeled by the thioether linkage of 4-chlorophenacyl-CoA. The two strands that form the A8 loop are shown in pink, and the C $\alpha$  position of the universally conserved glycine at position 409 is shown with a green sphere. The  $\beta$ -sheet-like interaction between Gly408-Gly409 and the  $\beta$ -alanine moiety of the pantetheine group is indicated with dashed lines. The interaction between His207 and Glu410 that stabilizes the A4 aromatic group (His207) in the new side chain position is shown with a red dashed line. The first turn of the helix at 251–265 is depicted transparently to allow the pantetheine chain to be seen.

that complement the structural characterization of the two conformations (57). Mutations were constructed in over 20 different residues of the 4CBL protein and were analyzed by steady-state kinetics. Rate constants were determined for the individual partial reactions for a subset of 10 of the mutant enzymes. The mutations were studied for their effects on  $k_1$  and  $k_2$ , the forward rate constants for the adenylation and thioesterification steps of the reaction. Not surprisingly, mutations in the ATP binding pocket had dramatic effects on  $k_1$ . Mutations in two residues that are located on the “thioester-forming face” of the C-terminal domain that stack against the adenine ring of CoA (Trp440 and Phe473) showed no effect on the adenylation partial reaction but 200-fold decreases in  $k_2$ , the rate of the thioester-forming partial reaction.

The most interesting results from this study relate to His207 and Glu410. His207 is conserved as an aromatic residue as part of the A4 motif (38). The precise identity of this residue correlates with the subfamily within the ANL family with NRPS adenylation domains most often containing a phenylalanine, small chain acyl-CoA synthetases containing a tryptophan, and larger chain acyl-CoA synthetases and luciferase enzymes containing a histidine. The His207 residue of 4CBL exhibits a side chain torsional rotation in the two observed crystal structures. In the adenylate-forming conformation, the side chain is rotated toward the acyl carboxylate with a side chain  $\chi_1$  torsion angle of  $-166^\circ$ . In the thioester-forming conformation, the  $\chi_1$  torsion angle is  $-60^\circ$ , with the side chain rotated away from the carboxylate (Figure 6). Upon further consideration, this initially minor observation provided one explanation for the catalytic advantage of the domain alternation strategy.

In the thioester-forming conformation of 4CBL, His207 forms a hydrogen bond with Glu410, which is located on the A8 loop and follows a universally conserved glycine residue (Gly409 in 4CBL). The His207 mutation resulted in a  $\sim 100$ -fold decrease in both the  $k_1$  and  $k_2$  rate constants. The Glu410 mutation had no effect on  $k_1$  but caused an 800-fold decrease in  $k_2$  despite the fact that this residue does not contact any of the reacting ligands. These results were interpreted to

demonstrate that the His207 played a role in both partial reactions, while the Glu410 residue played a role in only the thioester-forming step. The interaction between His207 and Glu410 in the second conformation (Figure 5, panel C) was seen to be highly important for stabilizing this state of the enzyme (9).

The A8 motif contains a conserved hinge residue, most commonly an aspartic acid but also commonly present as a lysine. This residue undergoes main chain torsion angle rotations that are responsible for the majority of the difference between the two conformations. Indeed, the main chain dihedral angles of the neighboring residues are not altered between the two studies (67). The dynamics of this hinge residue has been explored structurally and kinetically by mutation of the 4CBL hinge residue, Asp402, to a proline residue (67). The  $\phi/\psi$  angles of the proline residue allow the enzyme to adopt the adenylate-forming conformation; indeed, the crystal structure of the D402P mutant showed the overall fold of the enzyme was nearly identical to the wild-type enzyme in conformation I. The restraints imposed by the proline ring however prevent the enzyme from easily transitioning from conformation I to the thioester-forming conformation. Kinetic measurements showed that whereas the rate of the adenylation partial reaction was reduced  $\sim 3$ -fold, the rate constant for the thioester-forming reaction was reduced by 4 orders of magnitude.

**Catalytic Role of Domain Alternation.** Careful consideration of the structural and kinetic results provides insight into the role of the domain movement in the catalytic cycle. The side chain torsion of the A4 aromatic residue is conserved in the homologous crystal structures. In the adenylate-forming conformation, the A4 motif aromatic residue is located close to the carboxylate carbon where it positions this moiety to attack the  $\alpha$ -phosphate and displace  $PP_i$ . The  $\chi_1$  side chain torsion angle for the aromatic residue is  $-176 \pm 6^\circ$  in six members of the family that were crystallized in the adenylate-forming conformation bound with the adenylate intermediate or with ligands that mimic this state. Three exceptions were observed: the yeast Acs (46), human medium chain acyl-CoA synthetase (58), and the SrfA-C multidomain NRPS (31), all of which lack both AMP and the acyl substrate. Thus it appears that when the acyl-adenylate is present, the aromatic residue from the A4 motif is directed at the carboxylate. In contrast, in the thioester-forming state, the A4 aromatic residue is

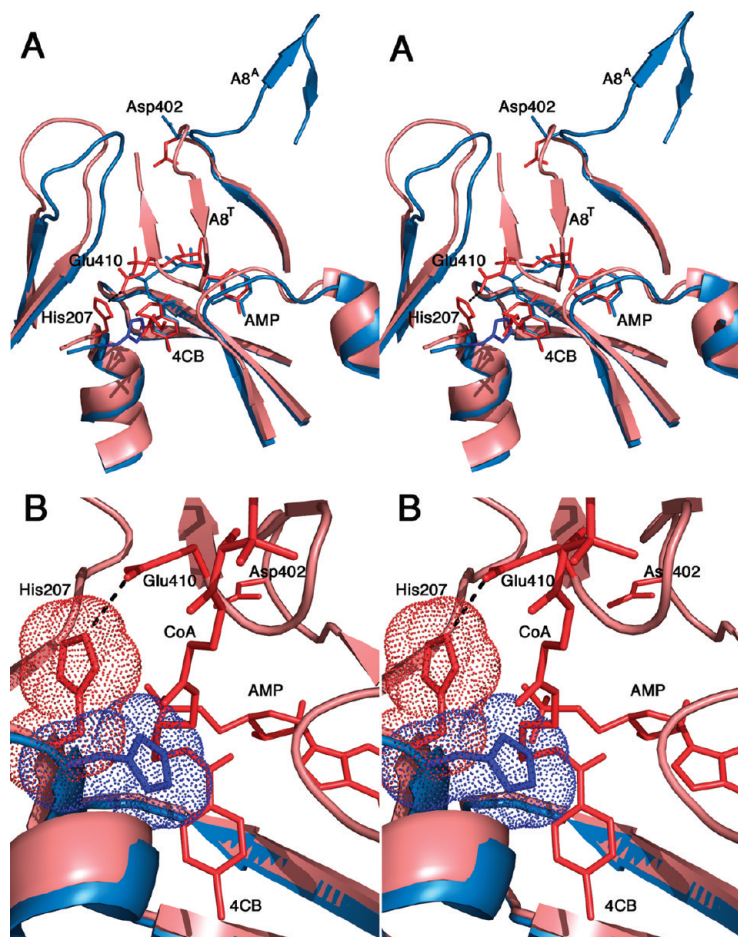


**Figure 6.** Impact of domain alternation on the orientation of the A4 aromatic residue. **A)** Superposition of the crystal structures of 4CBL in both the adenylate-forming (3CW8, blue) and thioester-forming (3CW9, pink) conformations. The view is oriented so that the reader is looking down the pantetheine tunnel into the active site. The A8 loop is shown in both conformations, indicated by the superscript (A8<sup>A</sup> and A8<sup>T</sup> for the adenylate- and thioester-forming conformations, respectively). The 4-chlorobenzoyl adenylate (blue) and the 4-chlorophenacyl thioester and AMP (red) are shown. The terminal  $\beta$ -alanine and cysteamine groups of the pantetheine chain are shown. In the thioester-forming conformation, the A8 loop rotates into the active site (A8<sup>T</sup>), where Glu410 interacts with His207 to rotate the side chain away from the 4CB molecule. **B)** Closer view of the active site. The orientation is rotated slightly from panel A, allowing observation of more of the pantetheine chain. The His207 side chain is shown with van der Waals surface. In the adenylate-forming structure, His207 occludes the pantetheine group from approaching the active site.

rotated out of the active site and exhibits an average  $\chi_1$  torsion angle of  $-59 \pm 14^\circ$  in six different structures.

Examining the structures of the family members that contain CoA provides an explanation for this necessary ro-

tation. The pantetheine tunnel is obstructed by the A4 aromatic residue in the side chain conformation observed in the adenylate-forming conformation (Figure 6). The rotation of the side chain allows the pantetheine group access to the carboxylate. The domain rotation brings the A8 loop into the active site where it provides an environment that promotes the rotation of the A4 aromatic residue to the  $-60^\circ$  side chain orientation. The specific environment that the A8 residues provide depends on the identity of the A4 residue. In proteins that contain an A4 histidine, a glutamic acid side chain is most commonly present on the A8 loop to form a hydrogen bond with the histidine imidazole group. In proteins that contain a phenylalanine or tryptophan A4 residue, the A8 loop more commonly contains a tyrosine or histidine that promotes the hydrophobic environment.

Thus, one role of the domain alternation appears to be to provide a new environment for the aromatic residue of the A4 motif to remove it from the pantetheine tunnel and allow access to the adenylate intermediate. Associated with this movement in the 4CBL enzyme, there are numerous residues on the thioester-specific face of the C-terminal domain that are involved in binding the CoA nucleotide (57). Two hydrophobic residues sandwich the nucleotide adenine ring. Interestingly, the two other protein structures containing CoA, the bacterial Acs (52) and the human medium chain acyl-CoA synthetase (58), both bind to CoA in a manner that is different from 4CBL and from each other. In both of these structures the CoA nucleotide does not interact with the mobile C-terminal domain.

Considering the chemical requirements for the partial reactions performed by this enzyme family, one can understand the role that domain alternation plays in the catalytic mechanism. The adenylation reaction requires the nucleophilic attack of the negatively charged carboxylate from the acyl substrate on the negatively charged  $\alpha$ -phosphate of ATP, displacing  $\text{PP}_i$ . To accomplish this reaction, the enzyme must properly orient the acyl substrate. The enzyme thus appears to use the A4 aromatic residue to constrict the substrate binding pocket, properly positioning the carboxylate for nucleophilic attack on the  $\alpha$ -phosphate. This required feature of the adenylation active site becomes a hindrance to the second partial reaction. In the thioester-forming reaction, the thiol of the CoA or pantetheine group must be able to approach the carboxylate carbon to displace the AMP leaving group and form the thioester linkage.

Domain alternation provides the A4 residue with an appropriate new environment to induce its rotation out of the active site.

The domain rotation also creates the pantetheine tunnel, appropriate to bind the thiol substrate. In all three CoA bound structures, the backbone residues on the A8 loop, the universally conserved glycine and the residue preceding it, hydrogen bond to the amide nitrogen of the  $\beta$ -alanine moiety of the pantetheine. Additionally, as noted above, the C-terminal domain also can contain residues that are involved in binding the CoA nucleotide (57).

The structures of these proteins also provide insights into the timing of the domain rotation with respect to the catalytic cycle. Recent structures of members of the ANL family bound to ATP (51, 58) confirms an earlier proposal (57) that the  $\beta$ - and  $\gamma$ -phosphates would bind in a cavity filled by the A8 loop in the thioester-forming conformation. This prediction of the location of the binding position of the phosphates assumed the inline displacement of the  $\text{PP}_i$  upon nucleophilic attack of the carboxylate on the  $\alpha$ -phosphate. The steric clash between the A8 loop and the  $\text{PP}_i$  binding pocket dictates that  $\text{PP}_i$  must be released prior to the domain rotation from the adenylate-forming to the thioester-forming conformation. Additionally, the rotation of the A4 aromatic residue suggests that the pantetheine group cannot bind productively to the enzyme in the adenylate-forming conformation. The aromatic side chain occludes the thiol of the pantetheine from approaching the active site and suggests that the domain rotation to the thioester-forming conformation must precede binding of CoA.

**Adenylation Domains of the Non-Ribosomal Peptide Synthetase.** Much structural and biochemical evidence exists for the domain alternation hypothesis in the acyl-CoA synthetases. Limited evidence supports a role in the A8 loop specifically in the thioester-forming reaction of the NRPS adenylation domains (66). Very recently the crystal structure of a four-domain NRPS was determined (31). The 1274 residue SrfA-C protein contains a full NRPS module organized as condensation, adenylation, peptidyl carrier, and thioesterase domains. This remarkable structure illustrated that the adenylation domain was positioned in a conformation that was similar, though not identical, to the adenylate-forming conformation (Figure 7, panel A). The C-terminal domain is rotated away from the N-terminal domain by  $\sim 40^\circ$  compared to the PheA structure, resulting in a more open active

site. The active site of the adenylation domain contains the amino acyl substrate leucine but does not contain AMP.

The PCP domain of the SrfA-C protein is positioned to interact productively with the upstream condensation domain (Figure 7, panel B). The serine residue on which the pantetheine would be placed was mutated to an alanine to produce homogeneous *apo*-protein. Nonetheless, the serine residue is close enough to the condensation domain active site that the structure observed is likely the conformation used in the condensation domain reaction. In contrast, the PCP domain is not positioned where it could donate the pantetheine arm to either the adenylation domain or the thioesterase domain. The authors note that a conformational rearrangement may be required to reposition the PCP to interact with the alternate catalytic sites. The C-terminal domain rotation of the adenylation domain was suggested as an attractive candidate to play a role in the progression of the nascent peptide from the active site of one catalytic domain to the next. Extensive interactions exist between the condensation domain and the N-terminal subdomain of the adenylation domain, which may serve as a “foundation” for each module. Upon completion of the adenylation partial reaction, the rotation of the C-terminal subdomain of the adenylation domain could be used to transport the pantetheine cofactor into the adenylation domain active site where it would become amino acylated in the thioesterification partial reaction using the conformation observed in Acs. Release of the loaded PCP domain, the thioester product of the adenylation domain complete reaction, would accompany a rotation of the adenylation C-terminal subdomain back to the conformation observed in PheA or SrfA-C. This would enable the delivery of the aminoacylated pantetheine cofactor to the upstream condensation domain for peptide bond formation. The conformational mechanism to direct the substrate to the downstream thioesterase domain remains to be determined.

This required domain rearrangement was modeled in a recent structural report of DltA (55). This structure was determined in the thioester-forming conformation bound to AMP. Extensive manual modeling was performed to generate a potential cycle of the DltA-catalyzed reaction (55). The reaction imitated in the unliganded, *apo*-state in which the C-terminal domain was in the open orientation seen in the original luciferase structure (39). The C-terminal domain of DltA was then

modeled into the orientation observed in PheA to mimic the adenylation partial reaction. The orientation of the triphosphates of modeled ATP is consistent with the subsequently determined structure of the human medium chain Acs bound to ATP (58). The structure of DltA in the thioester-forming conformation was also used to model the interaction of DltA with the carrier protein DltC using the pantetheine group from the structure of Acs (52). The other constraint used in modeling the interaction derived from the distance between the C-terminus of the adenylation domain and the N-terminus of the carrier protein, which we had suggested to be a maximum of 20–25 Å if the peptide linker were fully extended (66). This value was determined by comparison of the sequences of the linker joining the adenylation and PCP domains in multidomain NRPSs. In the structure of the SrfA-C multidomain NRPS, the distance between the termini is 14 Å.

Crystallographic studies of multidomain NRPS enzymes have been challenged by the difficulty in creating a conformationally uniform population of protein molecules. The SrfA-C structure does show the overall architecture of a complete termination module of an NRPS (31); however, it was necessary to mutate the phosphopantetheine binding site to obtain a uniform *apo* population of protein. Mutation of the hinge residue of the adenylation domains is one way to reduce the conformational flexibility of these large multidomain enzymes. The structure of the D402P mutant of 4CBL demonstrates that the proline mutation forces 4CBL to adopt the adenylate forming conformation (67). A similar mutation to the hinge of NRPS adenylation domains may be a useful tool for reducing the conformational flexibility of adenylation domains and may allow the crystallization of larger, multidomain NRPS proteins.

**Conformational Changes in Other Adenylating Enzymes.** The domain alternation hypothesis is presented as a strategy that enzymes of the ANL superfamily have adopted that allows them to catalyze the two-step adenylation and thioesterification reactions. As other ligases use an adenylation step to activate an acyl substrate, one might ask if other enzymes use a similar mechanism to stabilize the adenylation partial reaction and then allow the nucleophilic displacement of AMP in a second step.

A detailed description of other adenylate forming ligases, including amino acyl-tRNA synthetases (16, 68), NIS synthetases (17, 69), and ubiquitin ligases (70), is

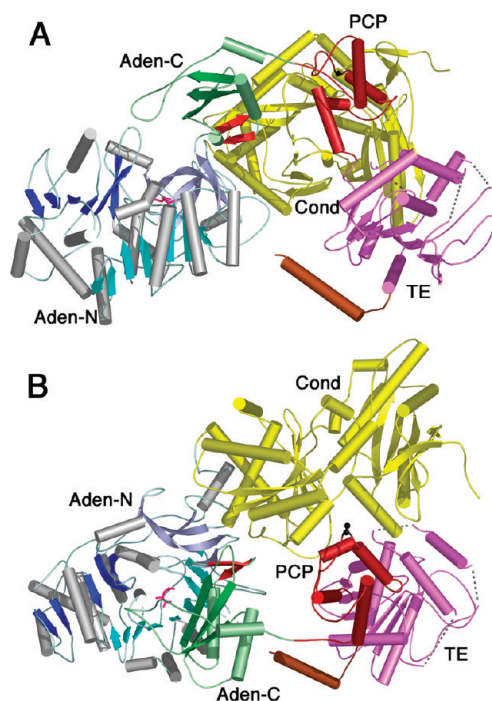


**Figure 7.** Crystal structure of the SrfA-C termination module from Surfactin NRPS cluster. The structure contains the domains organized as condensation-adenylation-PCP-thioesterase, from N- to C-terminus (2VSQ). The N-terminal domain is colored as other members of the ANL family with N-terminal domain containing  $\beta$ -sheets of blue and the C-terminal domain shown in green. The A8 loop is shown as the two-stranded  $\beta$ -sheet in red and a molecule of leucine is shown in pink in the adenylate-binding pocket. The condensation domain (yellow), PCP domain (red), and thioesterase domain (purple) are shown. The C-terminal purification tag formed a helix that is shown in brown. The cofactor binding site, Ser1003, was mutated to an alanine and is shown in black. In panel A, the adenylation domain is oriented as for other members of the ANL family in Figures 3 and 4. The C-terminal domain most closely represents the adenylate-forming conformation, although it is opened by  $\sim 40^\circ$  compared to other enzymes. In panel B, the image is rotated by  $\sim 90^\circ$  around the X-axis to depict the presentation of the cofactor binding site to the condensation domain active site cleft. The pantetheine cofactor is not present in the structure yet would be unable to reach the adenylation domain active site without a large conformational change.

beyond the scope of this Review. An analysis of the structures of multiple members of these families at different steps along the reaction coordinate identifies in some cases limited domain movements however the domain alternation strategy described for the ANL family of enzymes seems unique.

Why then have the ANL enzymes adopted the domain alternation catalytic strategy when other unrelated enzymes apparently accomplish similar chemistry without the dramatic conformational change? In these ligases, the energetically difficult step in the reaction is the initial nucleophilic attack of the carboxylate substrate on the  $\alpha$ -phosphate of ATP. The ATP is held firmly in place through specific interactions with the triphosphate, the ribose hydroxyls, and the adenine base. The challenge to the ligase then is to direct the carboxylate substrate to the  $\alpha$ -phosphate to promote the adenylate formation. It is reasonable to propose that the earliest members of the ANL enzyme superfamily were acyl-CoA synthetases that use chemically *uninteresting* fatty acids. Because the acyl substrates did not contain additional groups that the enzyme could use to position the carboxylate, the ANL enzymes evolved the A4 aromatic residue to position the carboxylate substrate and use domain alternation to allow access to this atom in the thioester-forming reaction.

The enzyme ligases mentioned above do not require a domain alternation strategy because their carboxylate substrates (amino acids in amino acyl-tRNA synthetases, di- or tricarboxylate compounds such as citrate or  $\alpha$ -ketoglutarate in the NIS synthetases, or protein molecules for ubiquitin ligases) contain numerous functional groups that can provide specific binding interactions between the adenylating enzyme and the nucleophilic substrate. The presence of these groups obviates the need to tightly surround the carboxylate carbon, leaving this atom accessible for attack in the second partial reaction. Even the glycyl-tRNA<sup>Gly</sup> synthetase enzyme (71), which has a relatively simple amino acyl substrate, uses multiple interactions, including a hydrogen bond to the glycine  $\alpha$ -proton, to position the carboxylate substrate precisely. These multiple interactions leave the glycine carboxylate carbon open for attack by the tRNA acceptor chain in the second partial reaction.

**Summary.** The importance of dynamics and conformational changes to proteins is now well established and allows enzymes to shield reactive intermediates and to induce the alignment of substrates and reactive catalytic groups from the protein. Several examples of large-scale domain rotations have been described that are distinct from the simple closing of catalytic loops that are often on the order of  $10\text{--}20^\circ$ . Generally, conformational changes that involve domain rotations larger than  $50^\circ$  are used to transport a substrate or intermedi-

ate between active sites. What makes the domain alteration of the ANL enzyme family unique is that this strategy allows the enzyme to present two different faces of a single protein domain to a single active site that catalyzes both reactions.

The extensive structural and functional investigations of the ANL enzyme family over the past decade have not only identified this catalytic strategy but have also explained the catalytic advantage that is derived from the use of the domain alternation. This is yet another example of the ways that enzymes continue to fascinate us with the ability to use unpredictable mechanisms to catalyze challenging chemical reactions. That this understanding explains observations first made over 40 years ago is particularly satisfying and points once again to the value of the complementary approaches of detailed kinetic and structural investigation.

Finally, the study of multiple members of this enzyme family has provided tremendous insights into the

catalytic cycle of the modular NRPS proteins. These assembly line proteins require the transfer of substrates between different catalytic domains and the recent structural advances demonstrate that the pantetheine cofactor is not sufficiently long to act solely as a swinging arm to transport the substrates. Instead, it appears that coordinated conformational movements are required to carry out this elaborate dynamic cycle. The domain alternation strategy of the NRPS adenylation domains is likely a necessary component of this modular protein family that ensures proper delivery of the bound intermediates to the catalytic domains.

*Acknowledgment:* I am very grateful to Drs. Debra Dunaway-Mariano, Courtney Aldrich, and Bruce Branchini for helpful comments and discussion throughout the course of our study of the ANL family of adenyating enzymes. I would also like to thank the members of my laboratory, Albert Reger, Eric Drake, Manish Shah, Jesse Sundlov, and Carter Mitchell, for their work on this project and their contributions made to the understanding of these enzymes. Work from my laboratory was supported in part by NIH grant GM-068440.

## REFERENCES

- McElroy, W. D., DeLuca, M., and Travis, J. (1967) Molecular uniformity in biological catalyses. The enzymes concerned with firefly luciferin, amino acid, and fatty acid utilization are compared, *Science* **157**, 150–160.
- Bar-Tana, J., and Rose, G. (1968) Studies on medium-chain fatty acyl-coenzyme a synthetase. Enzyme fraction I: mechanism of reaction and allosteric properties, *Biochem. J.* **109**, 275–282.
- Lipmann, F. (1944) Enzymatic synthesis of acetyl phosphate, *J. Biol. Chem.* **155**, 55–70.
- Berg, P. (1956) Acyl adenylates; an enzymatic mechanism of acetate activation, *J. Biol. Chem.* **222**, 991–1013.
- Farrar, W. W., and Plowman, K. M. (1975) Kinetics of acetyl-CoA synthetase-1. Mode of addition of substrates, *Int. J. Biochem.* **6**, 537–542.
- Kim, Y. S., and Kang, S. W. (1994) Steady-state kinetics of malonyl-CoA synthetase from *Bradyrhizobium japonicum* and evidence for malonyl-AMP formation in the reaction, *Biochem. J.* **297**, (2), 327–333.
- Li, H., Melton, E. M., Quackenbush, S., DiRusso, C. C., and Black, P. N. (2007) Mechanistic studies of the long chain acyl-CoA synthetase Faa1p from *Saccharomyces cerevisiae*, *Biochim. Biophys. Acta* **1771**, 1246–1253.
- Tian, Y., Suk, D. H., Cai, F., Crich, D., and Mesecar, A. D. (2008) *Bacillus anthracis* *o*-succinylbenzoyl-CoA synthetase: reaction kinetics and a novel inhibitor mimicking its reaction intermediate, *Biochemistry* **47**, 12434–12447.
- Wu, R., Cao, J., Lu, X., Reger, A. S., Gulick, A. M., and Dunaway-Mariano, D. (2008) Mechanism of 4-chlorobenzoate:coenzyme A ligase catalysis, *Biochemistry* **47**, 8026–8039.
- Babbitt, P. C., Kenyon, G. L., Martin, B. M., Charest, H., Slyvestre, M., Scholten, J. D., Chang, K. H., Liang, P. H., and Dunaway-Mariano, D. (1992) Ancestry of the 4-chlorobenzoate dehalogenase: analysis of amino acid sequence identities among families of acyl:adenyl ligases, enoyl-CoA hydratases/isomerases, and acyl-CoA thioesterases, *Biochemistry* **31**, 5594–5604.
- Turgay, K., Krause, M., and Marahiel, M. A. (1992) Four homologous domains in the primary structure of GrsB are related to domains in a superfamily of adenylate-forming enzymes, *Mol. Microbiol.* **6**, 529–546.
- Diez, B., Gutierrez, S., Barredo, J. L., van Solingen, P., van der Voort, L. H., and Martin, J. F. (1990) The cluster of penicillin biosynthetic genes. Identification and characterization of the pcbAB gene encoding the  $\alpha$ -aminoadipyl-cysteiny-valine synthetase and linkage to the pcbC and penDE genes, *J. Biol. Chem.* **265**, 16358–16365.
- Hori, K., Yamamoto, Y., Minetoki, T., Kurotsu, T., Kanda, M., Miura, S., Okamura, K., Furuyama, J., and Saito, Y. (1989) Molecular cloning and nucleotide sequence of the gramicidin S synthetase 1 gene, *J. Biochem. (Tokyo)* **106**, 639–645.
- Rusnak, F., Faraci, W. S., and Walsh, C. T. (1989) Subcloning, expression, and purification of the enterobactin biosynthetic enzyme 2,3-dihydroxybenzoate-AMP ligase: demonstration of enzyme-bound (2,3-dihydroxybenzoyl)adenylate product, *Biochemistry* **28**, 6827–6835.
- Gerlt, J. A., and Babbitt, P. C. (2001) Divergent evolution of enzymatic function: mechanistically diverse superfamilies and functionally distinct suprafamilies, *Annu. Rev. Biochem.* **70**, 209–246.
- Francklyn, C. S. (2008) DNA polymerases and aminoacyl-tRNA synthetases: shared mechanisms for ensuring the fidelity of gene expression, *Biochemistry* **47**, 11695–11703.
- Challis, G. L. (2005) A widely distributed bacterial pathway for siderophore biosynthesis independent of nonribosomal peptide synthetases, *ChemBioChem* **6**, 601–611.
- Fischbach, M. A., and Walsh, C. T. (2006) Assembly-line enzymology for polyketide and nonribosomal peptide antibiotics: logic, machinery, and mechanisms, *Chem. Rev.* **106**, 3468–3496.
- Kopp, F., and Marahiel, M. A. (2007) Where chemistry meets biology: the chemoenzymatic synthesis of nonribosomal peptides and polyketides, *Curr. Opin. Biotechnol.* **18**, 513–520.
- Walsh, C. T. (2008) The chemical versatility of natural-product assembly lines, *Acc. Chem. Res.* **41**, 4–10.
- Weissman, K. J., and Muller, R. (2008) Protein-protein interactions in multienzyme megasynthetases, *ChemBioChem* **9**, 826–848.

22. Lai, J. R., Koglin, A., and Walsh, C. T. (2006) Carrier protein structure and recognition in polyketide and nonribosomal peptide biosynthesis, *Biochemistry* 45, 14869–14879.
23. Mercer, A. C., and Burkart, M. D. (2007) The ubiquitous carrier protein—a window to metabolite biosynthesis, *Nat. Prod. Rep.* 24, 750–773.
24. MacCabe, A. P., van Liempt, H., Palissa, H., Unkles, S. E., Riach, M. B., Pfeifer, E., von Dohren, H., and Kinghorn, J. R. (1991)  $\delta$ -(L- $\alpha$ -Aminoacidipyl)-L-cysteinyl-D-valine synthetase from *Aspergillus nidulans*. Molecular characterization of the acvA gene encoding the first enzyme of the penicillin biosynthetic pathway, *J. Biol. Chem.* 266, 12646–12654.
25. Schofield, C. J., Baldwin, J. E., Byford, M. F., Clifton, I., Hajdu, J., Hensgens, C., and Roach, P. (1997) Proteins of the penicillin biosynthesis pathway, *Curr. Opin. Struct. Biol.* 7, 857–864.
26. Lai, J. R., Fischbach, M. A., Liu, D. R., and Walsh, C. T. (2006) Localized protein interaction surfaces on the EntB carrier protein revealed by combinatorial mutagenesis and selection, *J. Am. Chem. Soc.* 128, 11002–11003.
27. Lai, J. R., Fischbach, M. A., Liu, D. R., and Walsh, C. T. (2006) A protein interaction surface in nonribosomal peptide synthesis mapped by combinatorial mutagenesis and selection, *Proc. Natl. Acad. Sci. U.S.A.* 103, 5314–5319.
28. Frueh, D. P., Arthanari, H., Koglin, A., Vosburg, D. A., Bennett, A. E., Walsh, C. T., and Wagner, G. (2008) Dynamic thiolation-thioesterase structure of a non-ribosomal peptide synthetase, *Nature* 454, 903–906.
29. Koglin, A., Lohr, F., Bernhard, F., Rogov, V. V., Frueh, D. P., Strieter, E. R., Mofid, M. R., Guntert, P., Wagner, G., Walsh, C. T., Marahiel, M. A., and Dotsch, V. (2008) Structural basis for the selectivity of the external thioesterase of the surfactin synthetase, *Nature* 454, 907–911.
30. Koglin, A., Mofid, M. R., Lohr, F., Schafer, B., Rogov, V. V., Blum, M. M., Mittag, T., Marahiel, M. A., Bernhard, F., and Dotsch, V. (2006) Conformational switches modulate protein interactions in peptide antibiotic synthetases, *Science* 312, 273–276.
31. Tanovic, A., Samel, S. A., Essen, L. O., and Marahiel, M. A. (2008) Crystal structure of the termination module of a nonribosomal peptide synthetase, *Science* 321, 659–663.
32. Quadri, L. E. (2000) Assembly of aryl-capped siderophores by modular peptide synthetases and polyketide synthases, *Mol. Microbiol.* 37, 1–12.
33. Ferrer, J. L., Austin, M. B., Stewart, C., Jr., and Noel, J. P. (2008) Structure and function of enzymes involved in the biosynthesis of phenylpropanoids, *Plant Physiol. Biochem.* 46, 356–370.
34. Arora, P., Goyal, A., Natarajan, V. T., Rajakumara, E., Verma, P., Gupta, R., Yousuf, M., Trivedi, O. A., Mohanty, D., Tyagi, A., Sankaranarayanan, R., and Gokhale, R. S. (2009) Mechanistic and functional insights into fatty acid activation in *Mycobacterium tuberculosis*, *Nat. Chem. Biol.* 5, 166–173.
35. Trivedi, O. A., Arora, P., Sridharan, V., Tickoo, R., Mohanty, D., and Gokhale, R. S. (2004) Enzymic activation and transfer of fatty acids as acyl-adenylates in mycobacteria, *Nature* 428, 441–445.
36. Gehring, A. M., Mori, I., and Walsh, C. T. (1998) Reconstitution and characterization of the *Escherichia coli* enterobactin synthetase from EntB, EntE, and EntF, *Biochemistry* 37, 2648–2659.
37. Chang, K. H., Xiang, H., and Dunaway-Mariano, D. (1997) Acyl-adenylate motif of the acyl-adenylate/thioester-forming enzyme superfamily: a site-directed mutagenesis study with the *Pseudomonas* sp. strain CBS3 4-chlorobenzoate:coenzyme A ligase, *Biochemistry* 36, 15650–15659.
38. Marahiel, M. A., Stachelhaus, T., and Mootz, H. D. (1997) Modular peptide synthetases involved in nonribosomal peptide synthesis, *Chem. Rev.* 97, 2651–2674.
39. Conti, E., Franks, N. P., and Brick, P. (1996) Crystal structure of firefly luciferase throws light on a superfamily of adenylate-forming enzymes, *Structure* 4, 287–298.
40. Gocht, M., and Marahiel, M. A. (1994) Analysis of core sequences in the D-Phe activating domain of the multifunctional peptide synthetase TycA by site-directed mutagenesis, *J. Bacteriol.* 176, 2654–2662.
41. Martinez-Blanco, H., Reglero, A., Rodriguez-Aparicio, L. B., and Luengo, J. M. (1990) Purification and biochemical characterization of phenylacetyl-CoA ligase from *Pseudomonas putida*. A specific enzyme for the catabolism of phenylacetic acid, *J. Biol. Chem.* 265, 7084–7090.
42. Conti, E., Stachelhaus, T., Marahiel, M. A., and Brick, P. (1997) Structural basis for the activation of phenylalanine in the non-ribosomal biosynthesis of gramicidin S, *EMBO J* 16, 4174–4183.
43. Branchini, B. R., Murtiashaw, M. H., Magyar, R. A., and Anderson, S. M. (2000) The role of lysine 529, a conserved residue of the acyl-adenylate-forming enzyme superfamily, in firefly luciferase, *Biochemistry* 39, 5433–5440.
44. Horswill, A. R., and Escalante-Semerena, J. C. (2002) Characterization of the propionyl-CoA synthetase (PpE) enzyme of *Salmonella enterica*: residue Lys592 is required for propionyl-AMP synthesis, *Biochemistry* 41, 2379–2387.
45. May, J. J., Kessler, N., Marahiel, M. A., and Stubbs, M. T. (2002) Crystal structure of DhbE, an archetype for aryl acid activating domains of modular nonribosomal peptide synthetases, *Proc. Natl. Acad. Sci. U.S.A.* 99, 12120–12125.
46. Jogl, G., and Tong, L. (2004) Crystal structure of yeast acetyl-coenzyme A synthetase in complex with AMP, *Biochemistry* 43, 1425–1431.
47. Gulick, A. M., Lu, X., and Dunaway-Mariano, D. (2004) Crystal structure of 4-chlorobenzoate:CoA ligase/synthetase in the unliganded and aryl substrate-bound states, *Biochemistry* 43, 8670–8679.
48. Bains, J., and Boulanger, M. J. (2007) Biochemical and structural characterization of the paralogous benzoate CoA ligases from *Burkholderia xenovorans* LB400: defining the entry point into the novel benzoate oxidation (box) pathway, *J. Mol. Biol.* 373, 965–977.
49. Nakatsu, T., Ichiyama, S., Hiratake, J., Saldanha, A., Kobashi, N., Sakata, K., and Kato, H. (2006) Structural basis for the spectral difference in luciferase bioluminescence, *Nature* 440, 372–376.
50. Du, L., He, Y., and Luo, Y. (2008) Crystal structure and enantiomer selection by D-alanyl carrier protein ligase DltA from *Bacillus cereus*, *Biochemistry* 47, 11473–11480.
51. Osman, K. T., Du, L., He, Y., and Luo, Y. (2009) Crystal structure of *Bacillus cereus* D-alanyl carrier protein ligase (DltA) in complex with ATP, *J. Mol. Biol.* 388, 345–355.
52. Gulick, A. M., Starai, V. J., Horswill, A. R., Homick, K. M., and Escalante-Semerena, J. C. (2003) The 1.75 Å crystal structure of acetyl-CoA synthetase bound to adenosine-5'-propylphosphate and coenzyme A, *Biochemistry* 42, 2866–2873.
53. Bandarian, V., Patridge, K. A., Lennon, B. W., Huddler, D. P., Matthews, R. G., and Ludwig, M. L. (2002) Domain alternation switches B(12)-dependent methionine synthase to the activation conformation, *Nat. Struct. Biol.* 9, 53–56.
54. Hisanaga, Y., Ago, H., Nakagawa, N., Hamada, K., Ida, K., Yamamoto, M., Hori, T., Arii, Y., Sugahara, M., Kuramitsu, S., Yokoyama, S., and Miyano, M. (2004) Structural basis of the substrate-specific two-step catalysis of long chain fatty acyl-CoA synthetase dimer, *J. Biol. Chem.* 279, 31717–31726.
55. Yonus, H., Neumann, P., Zimmermann, S., May, J. J., Marahiel, M. A., and Stubbs, M. T. (2008) Crystal structure of DltA. Implications for the reaction mechanism of non-ribosomal peptide synthetase adenylation domains, *J. Biol. Chem.* 283, 32484–32491.
56. Shah, M. B., Ingram-Smith, C., Cooper, L. L., Qu, J., Meng, Y., Smith, K. S., Gulick, A. M. (2009) The 2.1 Å crystal structure of an acyl-CoA synthetase from *Methanosarcina acetivorans* reveals an alternate acyl binding pocket for small branched acyl substrates, *Proteins* Epub ahead of print; DOI: 10.1002/prot.22482.



57. Reger, A. S., Wu, R., Dunaway-Mariano, D., and Gulick, A. M. (2008) Structural characterization of a 140° domain movement in the two-step reaction catalyzed by 4-chlorobenzoate:CoA ligase, *Biochemistry* 47, 8016–8025.
58. Kochan, G., Pilka, E. S., von Delft, F., Oppermann, U., and Yue, W. W. (2009) Structural snapshots for the conformation-dependent catalysis by human medium-chain Acyl-coenzyme A synthetase ACSM2A, *J. Mol. Biol.* 388, 997–1008.
59. Goyal, A., Yousuf, M., Rajakumara, E., Arora, P., Gokhale, R. S., and Sankaranarayanan, R. (2006) Crystallization and preliminary X-ray crystallographic studies of the N-terminal domain of FadD28, a fatty-acyl AMP ligase from *Mycobacterium tuberculosis*, *Acta Crystallogr., Sect. F: Struct. Biol. Cryst. Commun.* 62, 350–352.
60. Reger, A. S., Carney, J. M., and Gulick, A. M. (2007) Biochemical and crystallographic analysis of substrate binding and conformational changes in acetyl-CoA synthetase, *Biochemistry* 46, 6536–6546.
61. Challis, G. L., Ravel, J., and Townsend, C. A. (2000) Predictive, structure-based model of amino acid recognition by nonribosomal peptide synthetase adenylation domains, *Chem. Biol.* 7, 211–224.
62. Rausch, C., Weber, T., Kohlbacher, O., Wohlleben, W., and Huson, D. H. (2005) Specificity prediction of adenylation domains in nonribosomal peptide synthetases (NRPS) using transductive support vector machines (TSVMs), *Nucleic Acids Res.* 33, 5799–5808.
63. Stachelhaus, T., Mootz, H. D., and Marahiel, M. A. (1999) The specificity-conferring code of adenylation domains in nonribosomal peptide synthetases, *Chem. Biol.* 6, 493–505.
64. Lautru, S., Deeth, R. J., Bailey, L. M., and Challis, G. L. (2005) Discovery of a new peptide natural product by *Streptomyces coelicolor* genome mining, *Nat. Chem. Biol.* 1, 265–269.
65. Branchini, B. R., Southworth, T. L., Murtiashaw, M. H., Wilkinson, S. R., Khattak, N. F., Rosenberg, J. C., and Zimmer, M. (2005) Mutagenesis evidence that the partial reactions of firefly bioluminescence are catalyzed by different conformations of the luciferase C-terminal domain, *Biochemistry* 44, 1385–1393.
66. Drake, E. J., Nicolai, D. A., and Gulick, A. M. (2006) Structure of the EntB multidomain nonribosomal peptide synthetase and functional analysis of its interaction with the EntE adenylation domain, *Chem. Biol.* 13, 409–419.
67. Wu, R., Reger, A. S., Lu, X., Gulick, A. M., and Dunaway-Mariano, D. (2009) The mechanism of domain alternation in the acyl-adenylate forming ligase superfamily member 4-chlorobenzoate:coenzyme A ligase, *Biochemistry* 48, 4115–4125.
68. Sekine, S., Nureki, O., Dubois, D. Y., Bernier, S., Chenevert, R., Lapointe, J., Vassilyev, D. G., and Yokoyama, S. (2003) ATP binding by glutamyl-tRNA synthetase is switched to the productive mode by tRNA binding, *EMBO J.* 22, 676–688.
69. Schmelz, S., Kadi, N., McMahan, S. A., Song, L., Oves-Costales, D., Oke, M., Liu, H., Johnson, K. A., Carter, L., Botting, C. H., White, M. F., Challis, G. L., and Naismith, J. H. (2009) Structure and function of AcsD a new class of adenyating enzyme that catalyzes enantioselective citrate desymmetrization in pathogenicity-conferring siderophore biosynthesis, *Nat. Chem. Biol.* 5, 174–182.
70. Lee, I., and Schindelin, H. (2008) Structural insights into E1-catalyzed ubiquitin activation and transfer to conjugating enzymes, *Cell* 134, 268–278.
71. Arnez, J. G., Dock-Bregeon, A. C., and Moras, D. (1999) Glycyl-tRNA synthetase uses a negatively charged pit for specific recognition and activation of glycine, *J. Mol. Biol.* 286, 1449–1459.